Combined Analysis of Cosmic-Ray Anisotropy with 5 years of IceCube data and 2 years of HAWC

Juan Carlos Díaz Vélez[a,b],
M. Ahlers[c], D. Fiorino[d], P. Desiati[b]

Solvay workshop on SUGAR 2018
Brussels, 23-26 January

[a]Centro Universitario de los Valles, Universidad de Guadalajara, Guadalajara, Jalisco, México
[b]Wisconsin IceCube Particle Astrophysics Center (WIPAC) and Department of Physics, University of Wisconsin–Madison, Madison, WI 53706, USA
[c]Niels Bohr Institute, University of Copenhagen, Copenhagen, Denmark
[d]Department of Physics, University of Maryland, College Park, MD, USA

Universidad de Guadalajara
Centro Universitario de los Valles

Over the last few decades, several studies have measured a large scale anisotropy at 10^{-3} level and a small-scale structure with an amplitude of 10^{-4} and angular size from 10° to 30°.

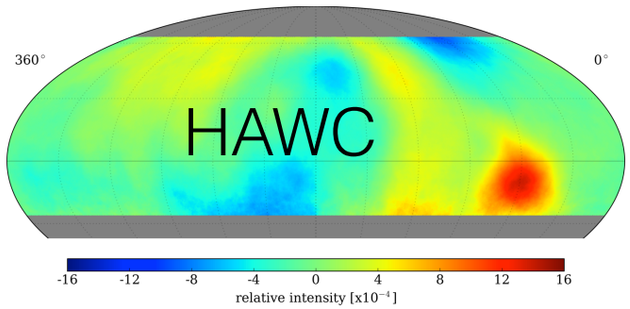

A. U. Abeysekara et al. Astrophys. J. (2014)

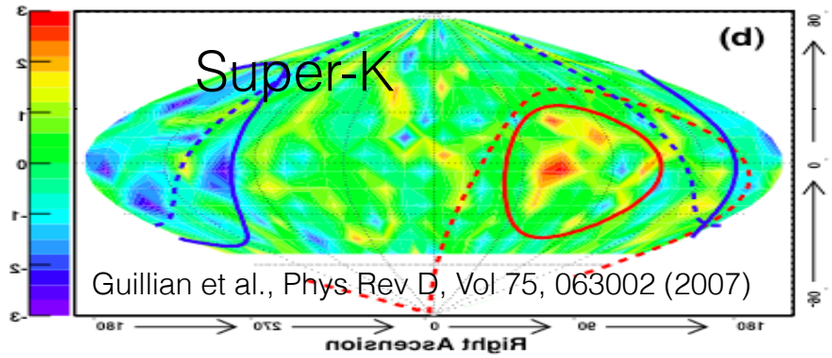

Guillian et al., Phys Rev D, Vol 75, 063002 (2007)

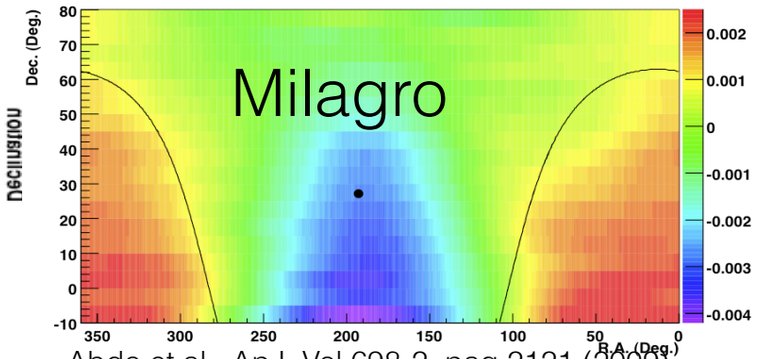

Abdo et al., ApJ, Vol 698-2, pag 2121 (2009)

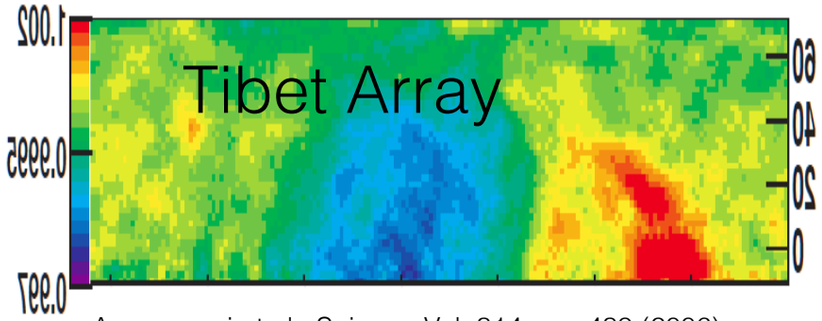

Amenomori et al., Science Vol. 314, pp. 439 (2006)

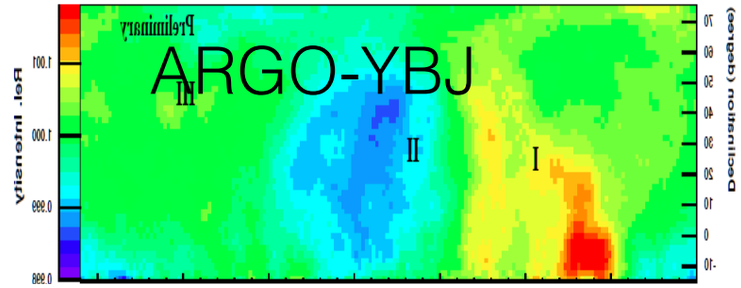

Zhang et al. Proc. 32nd ICRC (2009)

North

South

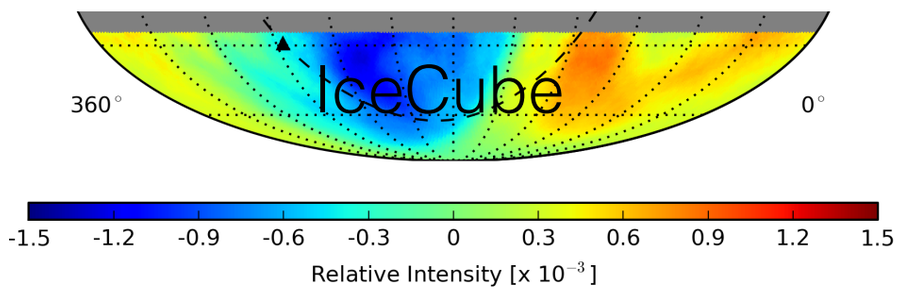

M. G. Aartsen et al. Astrophys.J. 826 (2016)

Large-scale features in South appear to be a continuation of those observed in the Northern Hemisphere.

Method for measuring CR anisotropy

1 Build a binned data map using the equatorial coordinates of the events

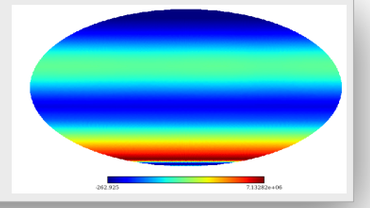

2 Construct a “reference” map by integrating acceptance over 24 hours.

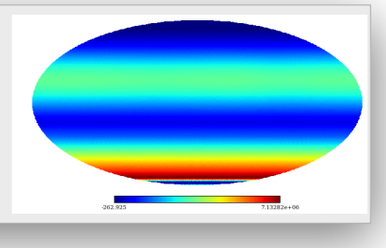

Time-scrambling: $(\theta, \phi, t) \rightarrow (\alpha, \delta)$

$(\theta, \phi, t') \rightarrow (\alpha', \delta')$

Direct integration: $\langle N(\alpha, \delta) \rangle = \int dt \int d\Omega A(ha, \delta) \cdot R(t) \cdot \epsilon(ha, \alpha, t)$

3 Correlate pixels to increase sensitivity to different angular scales

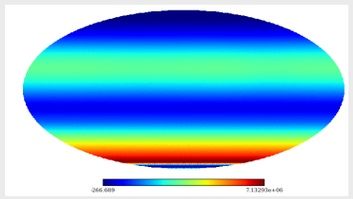

Relative Intensity

$$\delta I(\alpha, \delta)_i = \frac{N(\alpha, \delta)_i - \langle N \rangle(\alpha, \delta)_i}{\langle N \rangle(\alpha, \delta)_i}$$

4 Calculate relative differences between data and reference with significance.

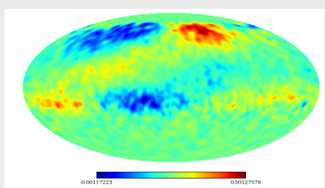

$$s_i = \sqrt{2} \left\{ N_i \log \left[\frac{1+\alpha}{\alpha} \left(\frac{N_i}{N_i + N_o} \right) \right] + N_o \log \left[(1+\alpha) \left(\frac{N_o}{N_i + N_o} \right) \right] \right\}^{1/2}$$

5 Calculate statistical significance for each pixel

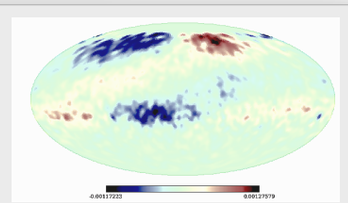

Field of view and reference map

- Traditional time-integration methods can strongly attenuate large-scale structures exceeding the size of the instantaneous field of view for detectors located at mid latitudes.

- A fixed position on the celestial sphere is only observable over a limited period every day. The total number of cosmic ray events from a fixed position can only be compared against reference data observed during the same period.

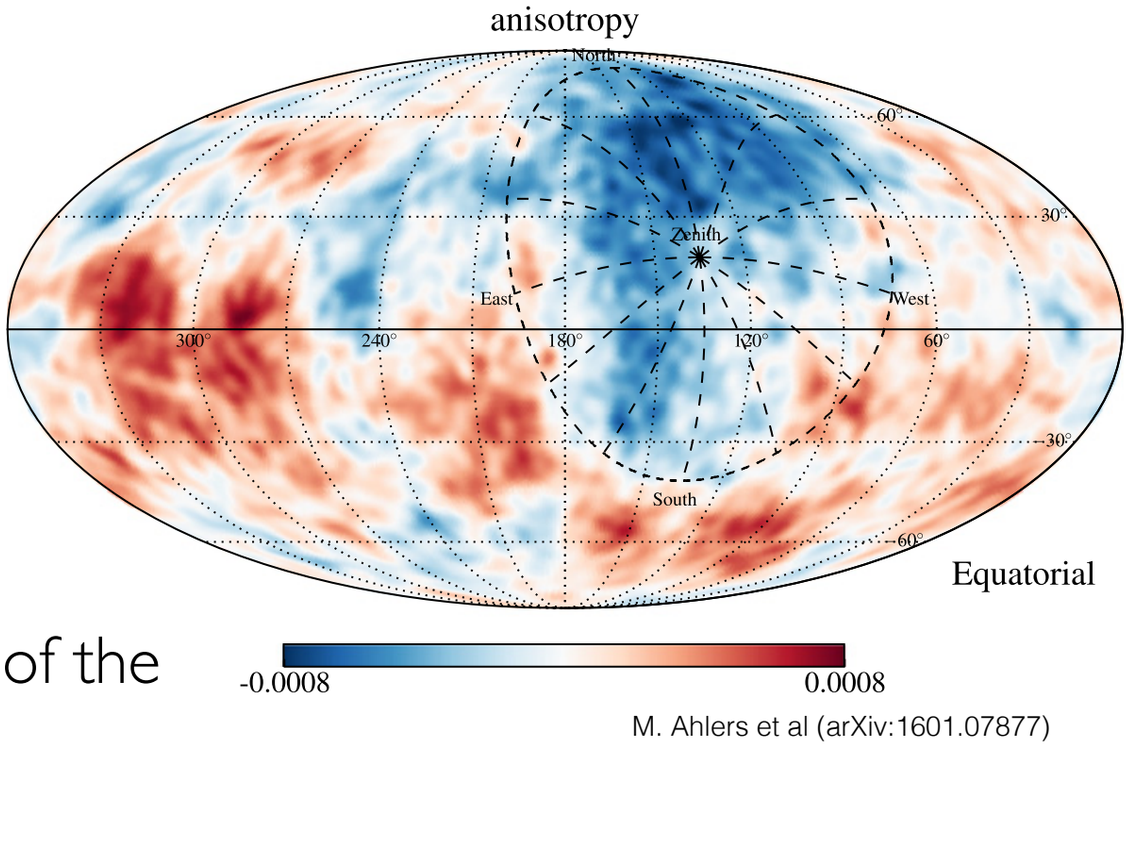

- This can lead to an under- or overestimation of the isotropic reference level.

Iterative maximum likelihood method

Ahlers, BenZvi, Desiati, Díaz-Vélez, Fiorino, Westerhoff (arXiv:1601.07877)

The likelihood of observing n cosmic rays is given by the product of Poisson probabilities

$$\mathcal{L}(n|I,\mathcal{N},\mathcal{A}) = \prod_{\tau i} \frac{(\mu_{\tau i})^{n_{\tau i}} e^{-\mu_{\tau i}}}{n_{\tau i}!} ,$$

relative intensity

relative acceptance

$$\mu_{\tau i} \simeq I_{\tau i} \mathcal{N}_{\tau} \mathcal{A}_i$$

expected number of events from isotropic background

Maximize the likelihood ratio via null hypothesis in N, A y I

$$\lambda = \frac{\mathcal{L}(n|I,\mathcal{N},\mathcal{A})}{\mathcal{L}(n|I^{(0)},\mathcal{N}^{(0)},\mathcal{A}^{(0)})}$$

maximum values ($I^{\star}$,$N^{\star}$,$A^{\star}$) must follow

$$I^{\star}_{a} = \sum_{\tau} n_{\tau a} \Big/ \sum_{\kappa} \mathcal{A}^{\star}_{\kappa a} \mathcal{N}^{\star}_{\kappa} ,$$

$$\mathcal{N}^{\star}_{\tau} = \sum_{i} n_{\tau i} \Big/ \sum_{j} \mathcal{A}^{\star}_{j} I^{\star}_{\tau j} ,$$

$$\mathcal{A}^{\star}_{i} = \sum_{\tau} n_{\tau i} \Big/ \sum_{\kappa} \mathcal{N}^{\star}_{\kappa} I^{\star}_{\kappa i} ,$$

which can be solved iteratively.

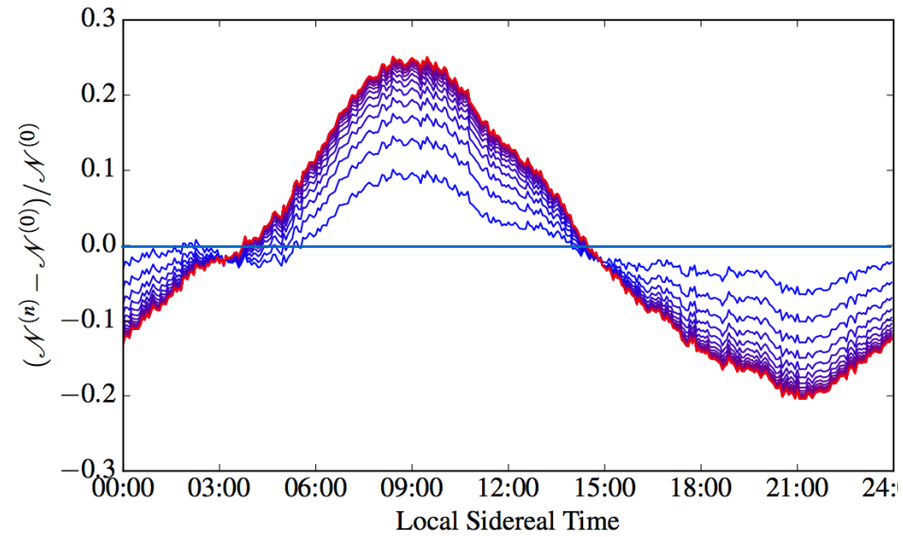

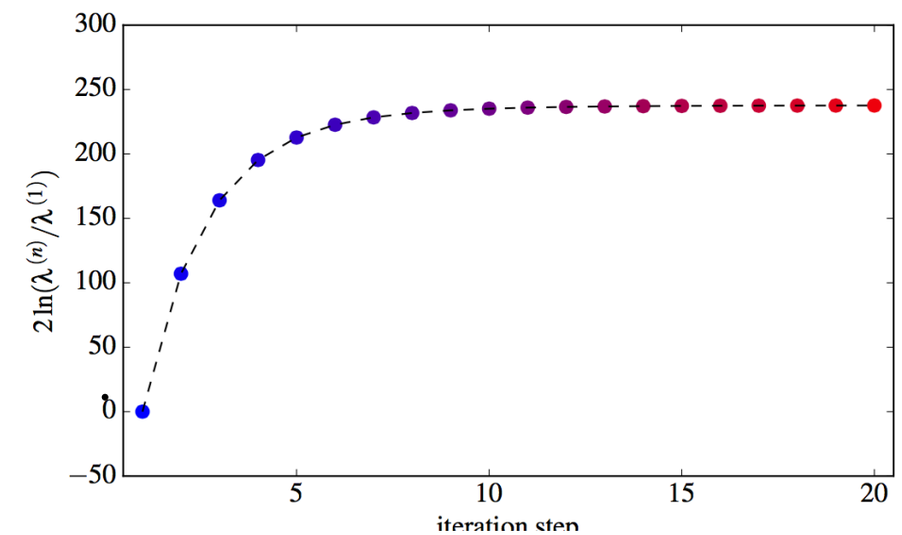

The HAWC Observatory

The HAWC Observatory

HAWC
High Altitude Water Cherenkov
Gamma-Ray Observatory

Mapping the Northern Sky in High-Energy Gamma Rays

HAWC Observatory

HAWC operates day and night, providing a large field of view for the observation of the highest energy gamma rays.

Pico de Orizaba
(5,626 m)

HAWC is located at 4,100 m above sea level, covering an area of 20,000 m^2.

150 m

Water Cherenkov tank

HAWC comprises an array of 300 tanks that record the particles created in gamma-ray and cosmic-ray showers.

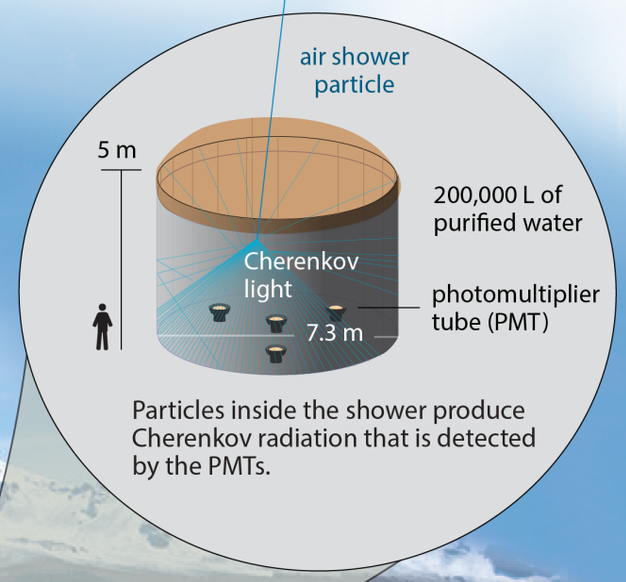

Particles inside the shower produce Cherenkov radiation that is detected by the PMTs.

Gamma rays vs cosmic rays

HAWC selects gamma rays from among a much more abundant background of cosmic rays.

gamma-ray shower	cosmic-ray shower
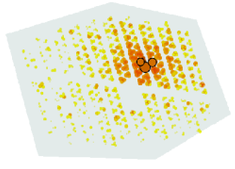	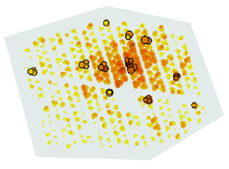
"hot" spots concentrate around the core	"hot" spots are more dispersed

The IceCube Observatory

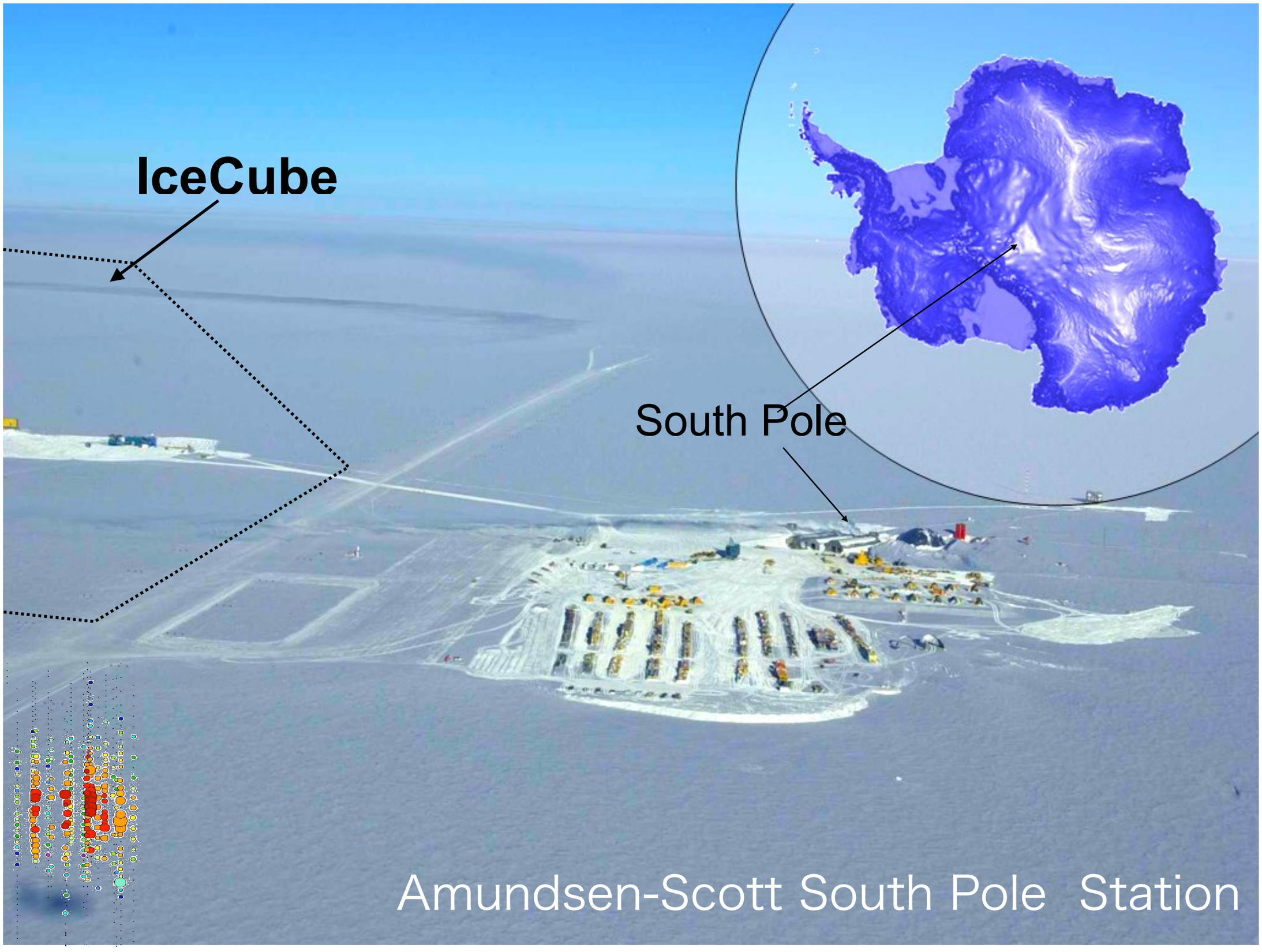

The IceCube Observatory

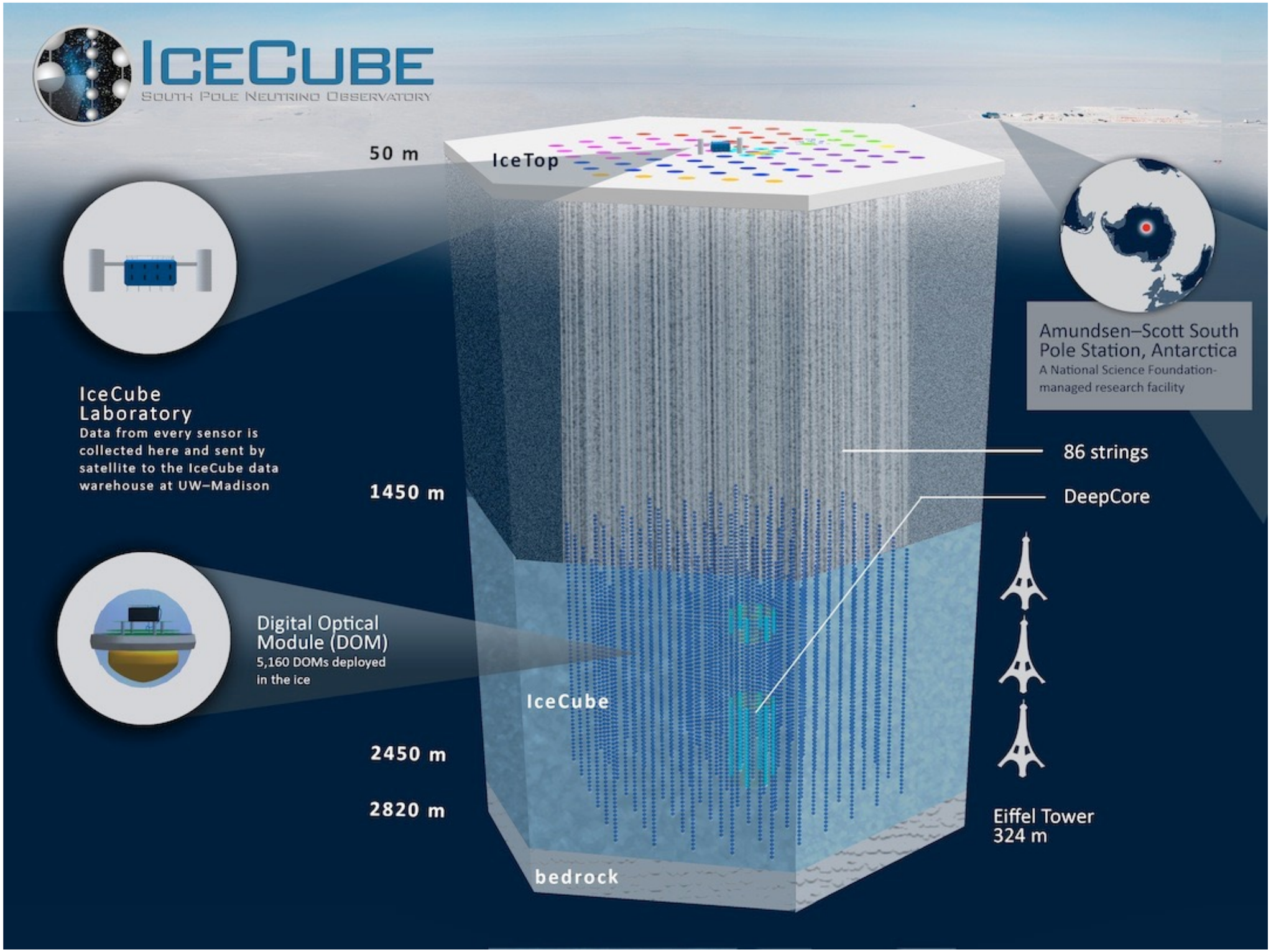

The IceCube and HAWC Data Sets

Individual experiments have provided partial sky coverage that limits the interpretation of the results. This first full-sky combined observation at the same energy is done with two observatories covering most of the celestial sphere.

	IceCube		**HAWC**	
Hemisphere	Southern		Northern	
Latitude	-90°		19°	
Detection method	muons produced by CR		air showers produced by CR and γ	
Field of view	-90°/-20°, ~4 sr (same sky over 24h)		-30° /68° , ~2 sr (8 sr observed)/24 h	
Livetime	5 years		519 days over a period of 653 days	
Detector trigger rate	2.5 kHz		25 kHz	
	quality cuts	energy cuts	quality cuts	energy cuts
Median primary energy	20 TeV	10 TeV	2 TeV	10 TeV
Approx. angular	2-3°	2-6°	0.3-1.5°	0.3-1.5°
Events	2.8×10^{11}	1.7×10^{11}	7.1×10^{10}	2.8×10^{10}

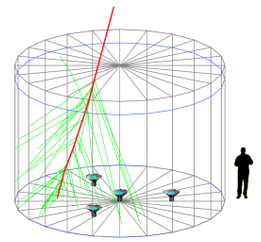

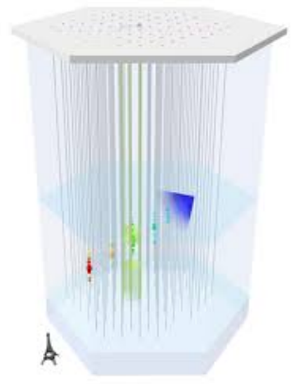

Data selected for analysis come from IC86 2011-2015, as well as 2 years of HAWC in its final configuration of 300 tanks (HAWC300). Only continuous sidereal days* of data were chosen for these analyses in order to reduce the bias of uneven exposure along right ascension.

* Gaps of 20 min. allowed within each 24 h period

Energy Distribution

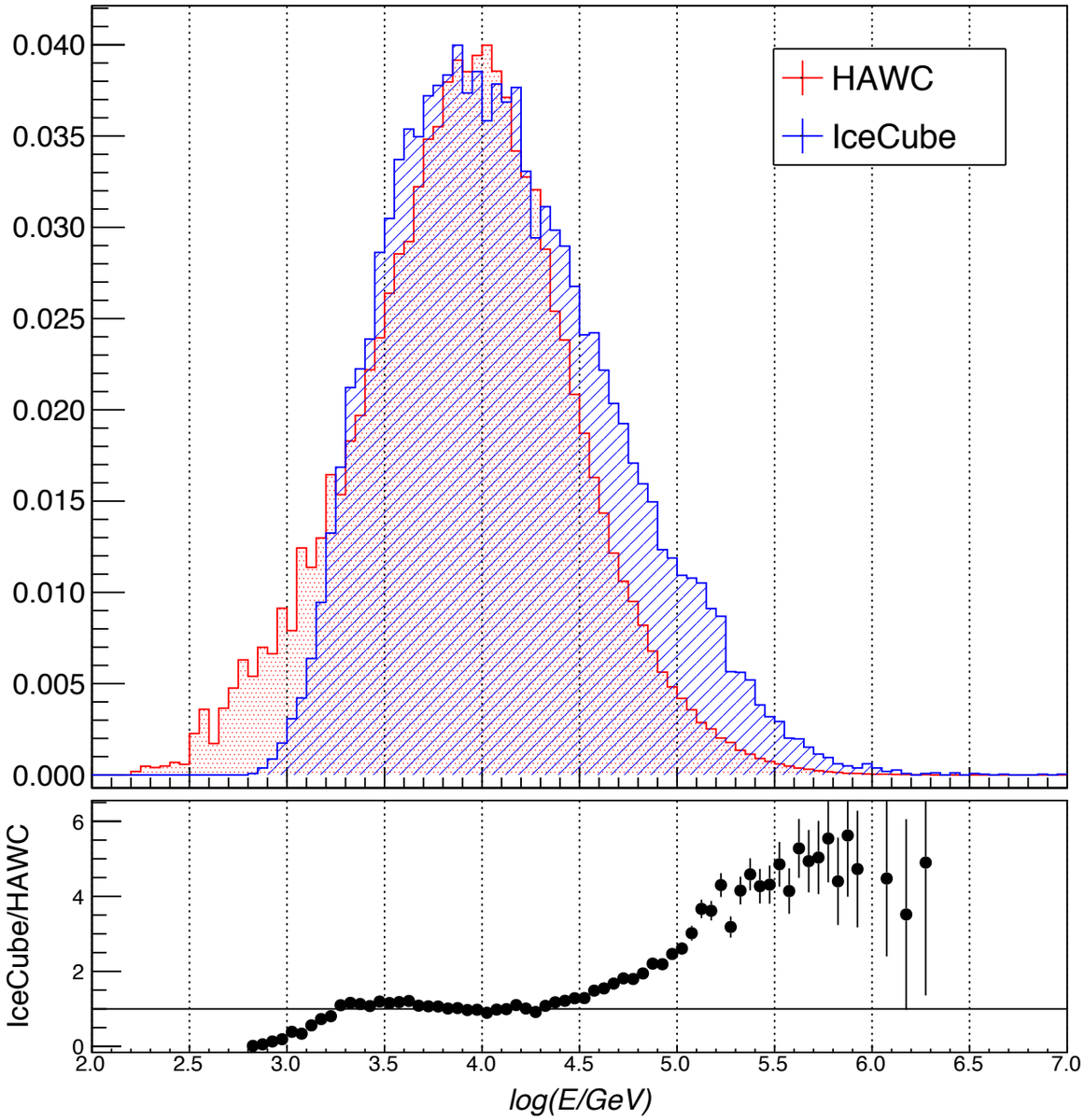

Composition

	IceCube	HAWC
Proton	0.756	0.616
He	0.195	0.311
CNO	0.028	0.047
NeMgSi	0.013	0.019
Fe	0.008	0.008

Median Energy

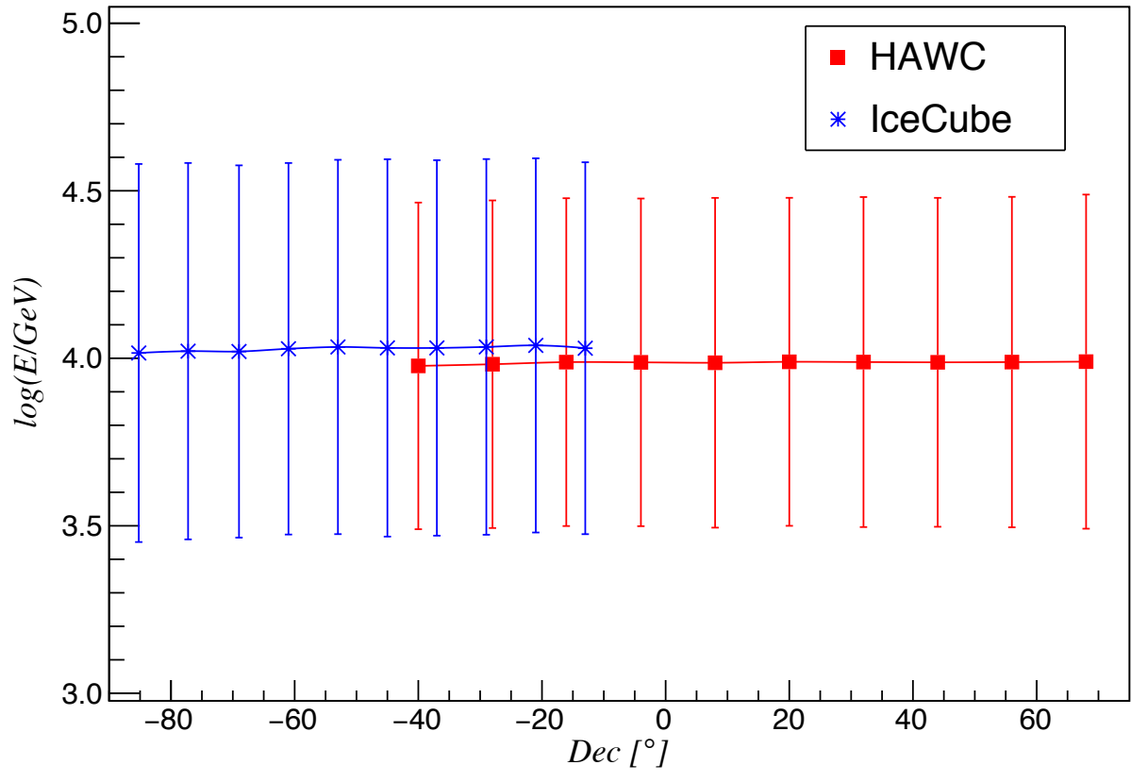

The resulting energy distribution of the two datasets after applying energy cuts is shown on the left above. After cuts, both CR data sets have a median energy of approximately 10 TeV with little dependence on zenith angle. Before cuts, the median energy grows as a function of shower zenith angle and is largest in the narrow region of overlap between the two detectors.

The IceCube and HAWC Data Sets

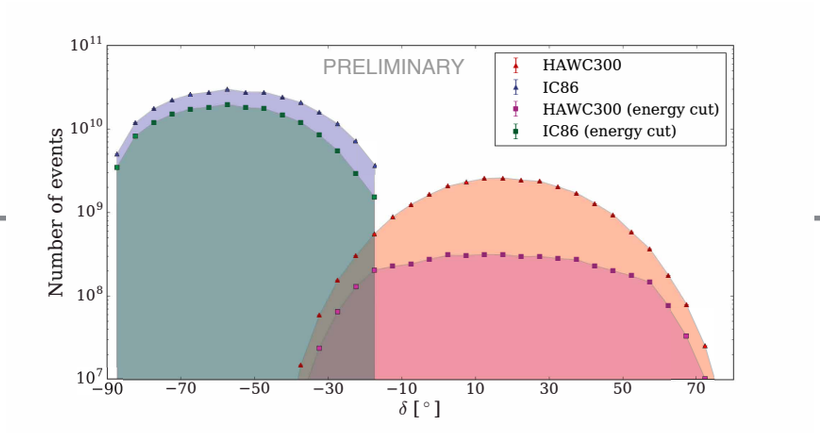

Distribution of events as a function of declination for IceCube and HAWC. Triangles correspond to the full energy spectrum and squares correspond to the same datasets after applying energy cuts.

HAWC Data Coverage

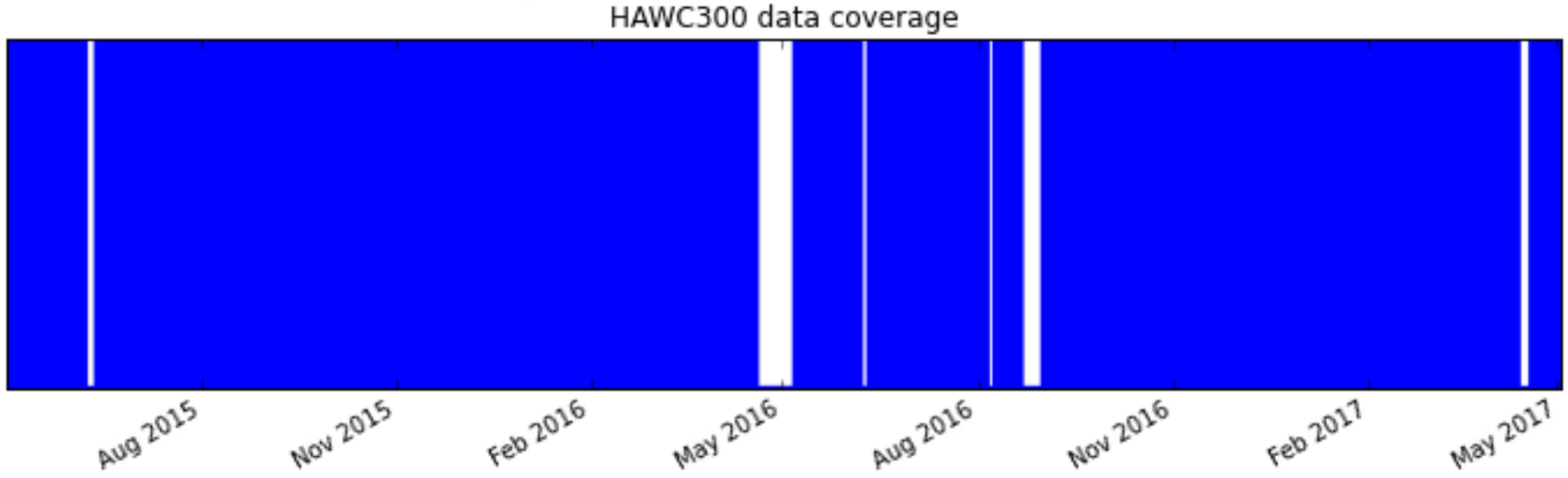

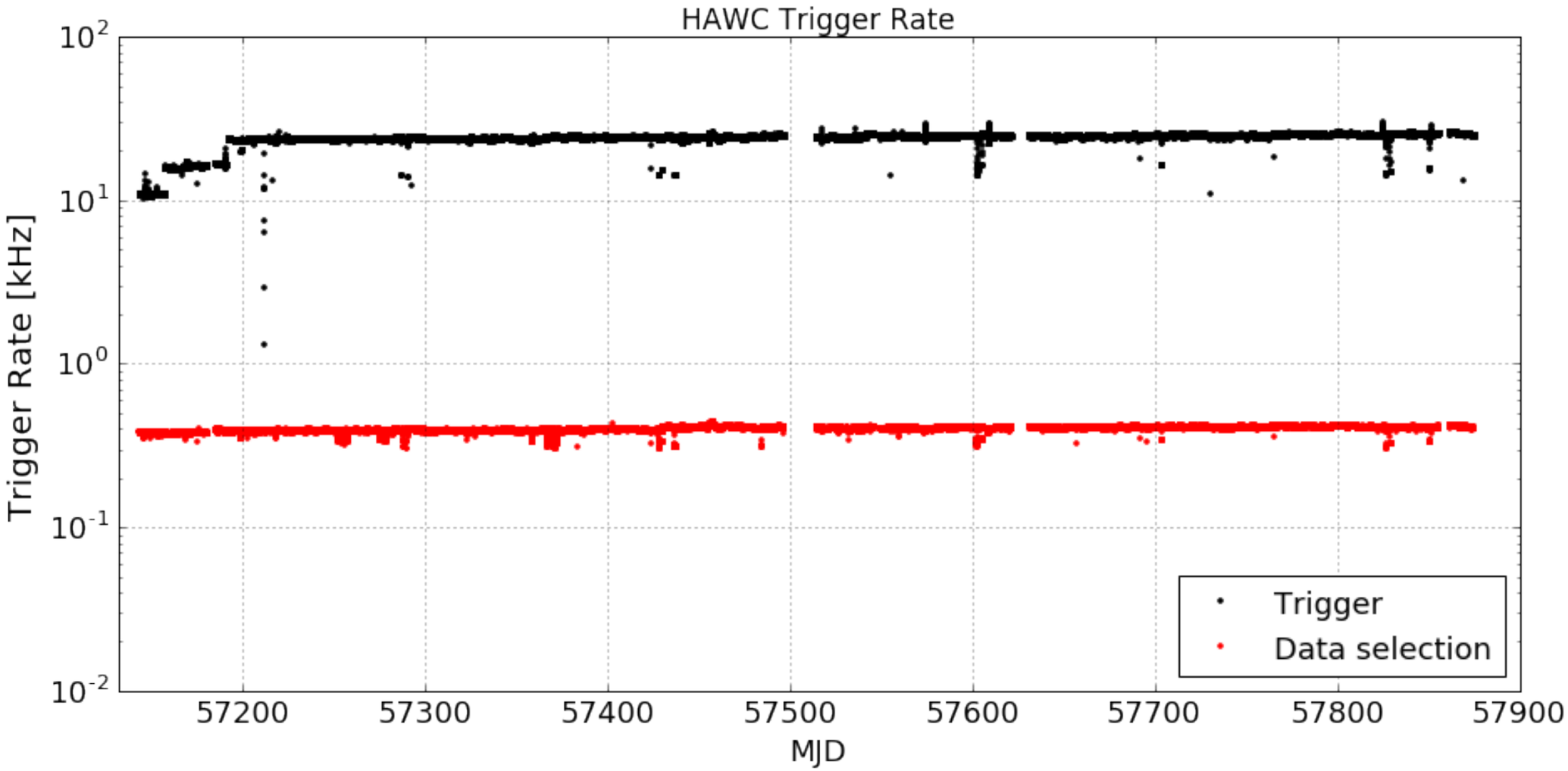

Atmospheric pressure correction

Atmospheric tides:

- Lunar gravitational tides.
- Thermally driven tides: heating associated with solar radiation. Dynamics determined by both the Coriolis force and gravity. (X. Zhang, et a. J. Geoph. Res.: Space Physics (2010))

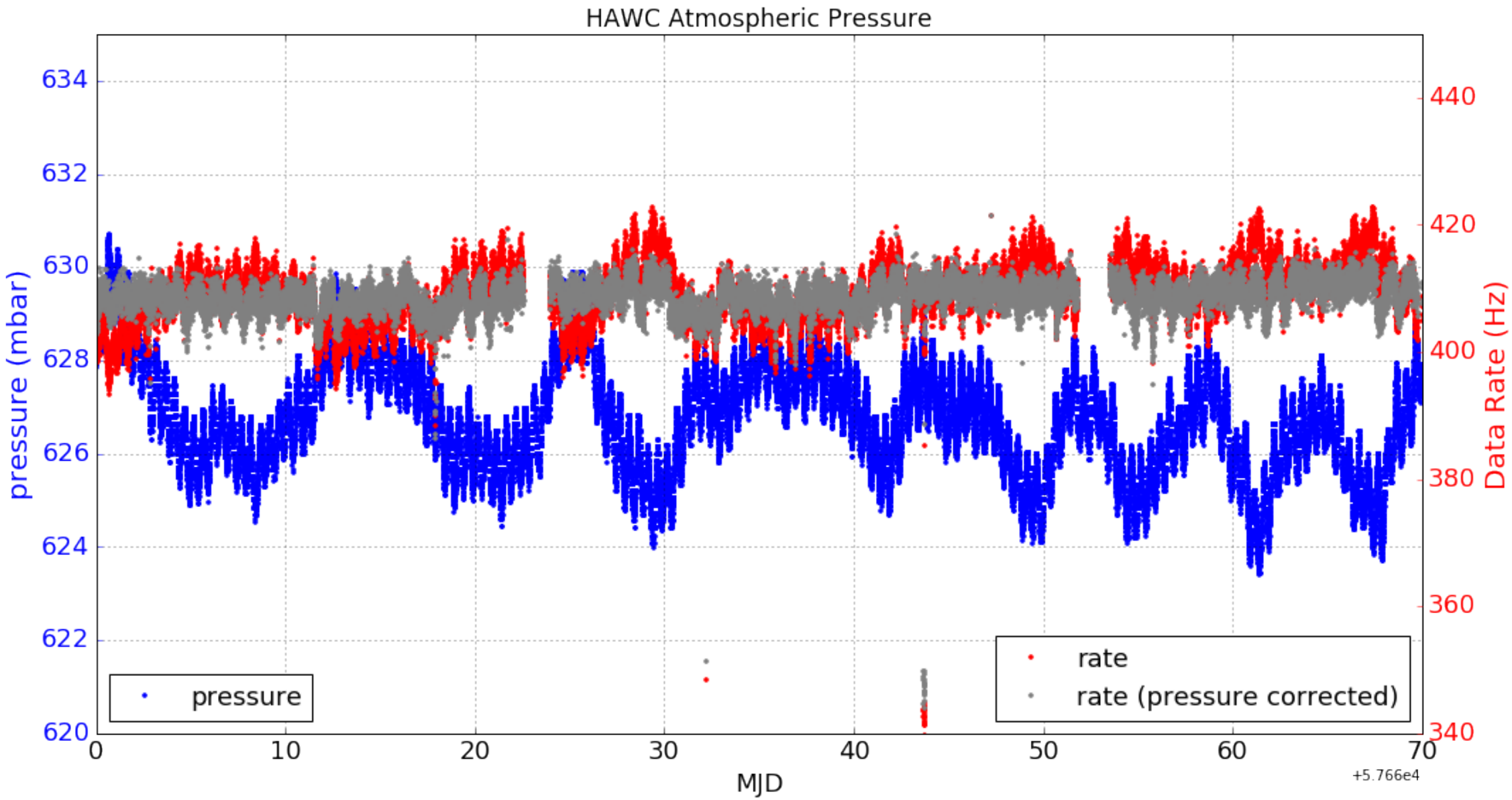

Solar dipole correction (HAWC)

Relative movement of the Earth in the solar system

$$\frac{\Delta I}{\langle I \rangle} = (\gamma + 2)\frac{v}{c}\cos(\theta_v)$$

A weight is added to each event to correct the solar dipole and atmospheric variations.

The difference is small compared to statistical errors.

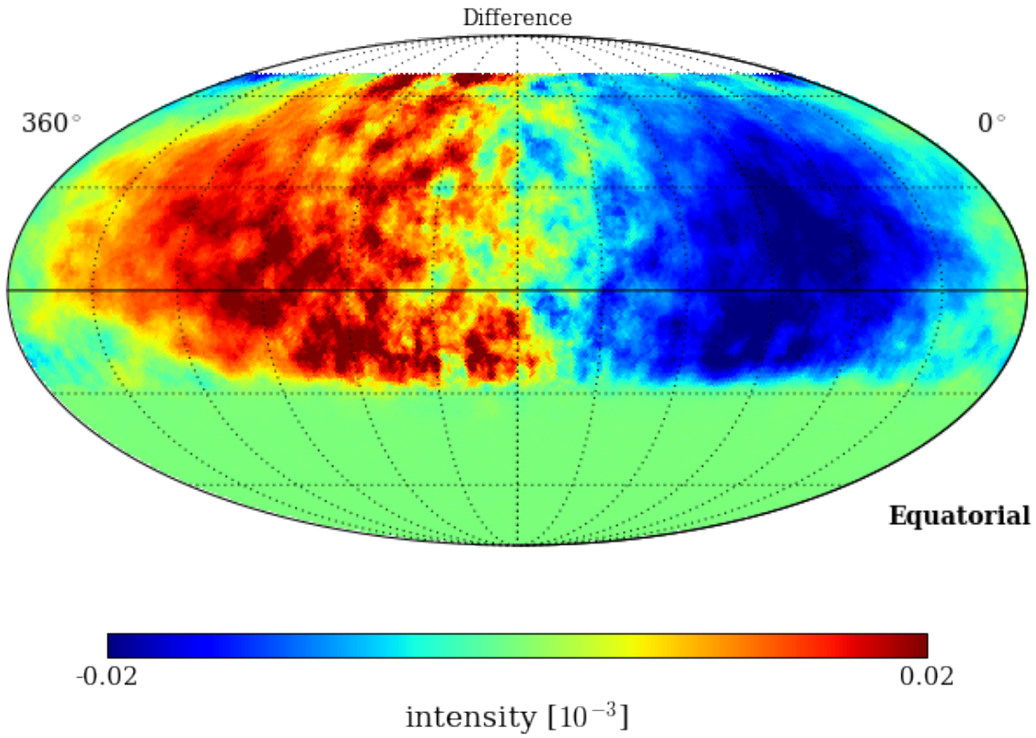

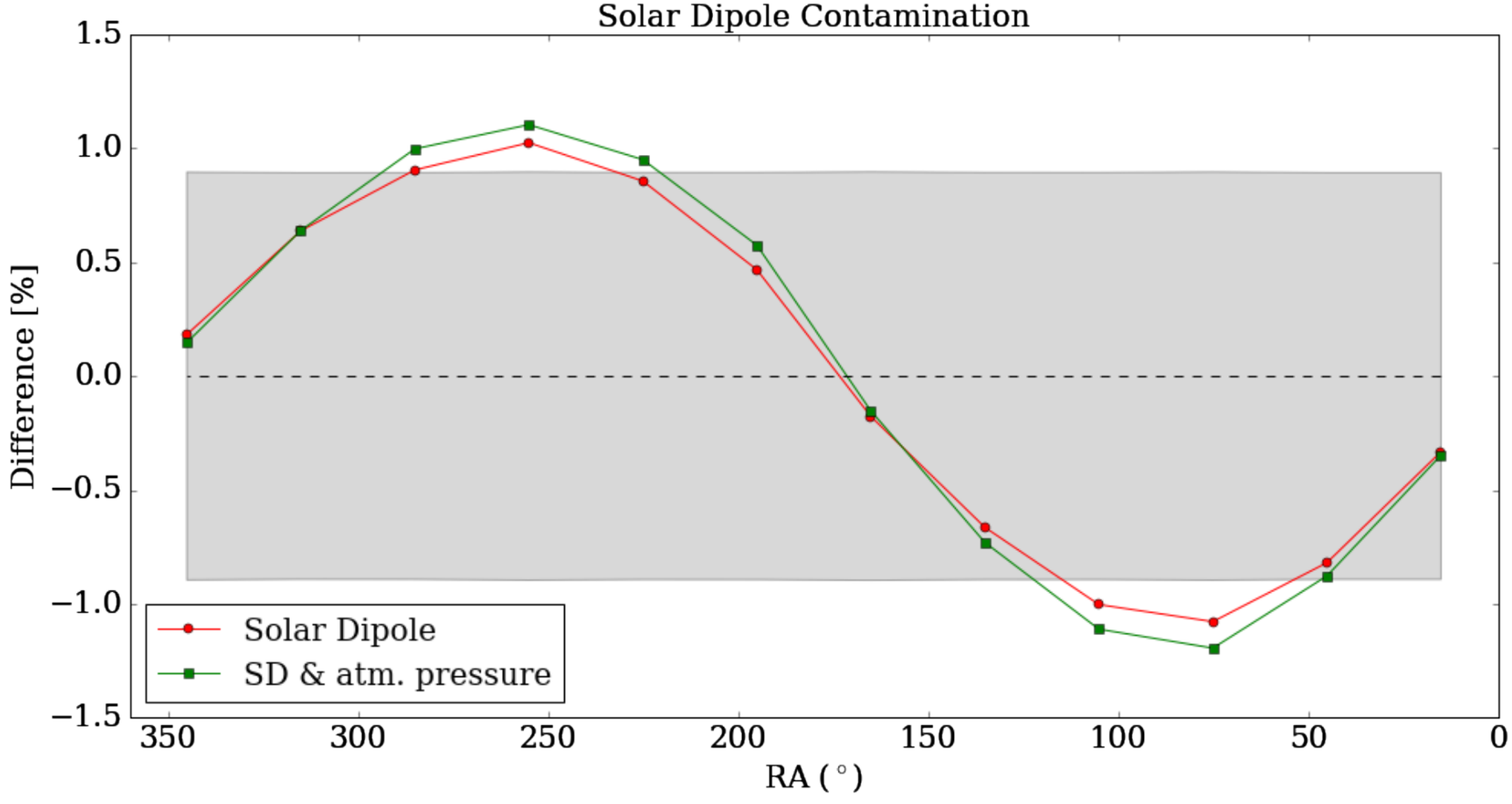

Seasonal variations in IceCube

- Modulations in IceCube trigger rates have an annual period since the solar cycle in the South Pole has 365 days instead of 24 hours.
- In IceCube there are also atmospheric variations of higher frequency (and lower amplitude) but these affect the event rate simultaneosuly in all directions of azimuth.
- While IceCube muon rate is sensitive to variation in T_{eff}, it is generally insensitive to surfafe pressure changes.

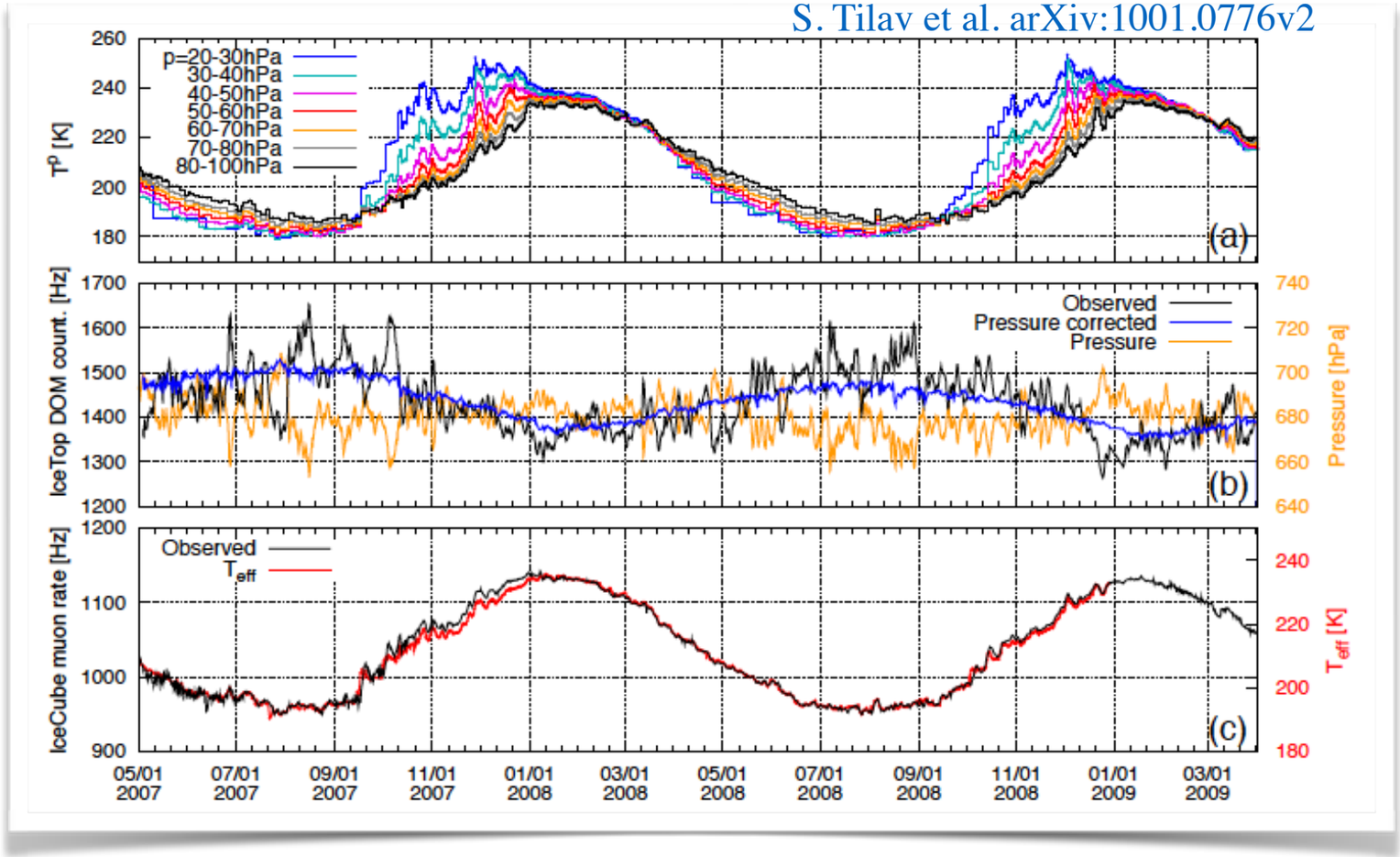

Horizontal projection

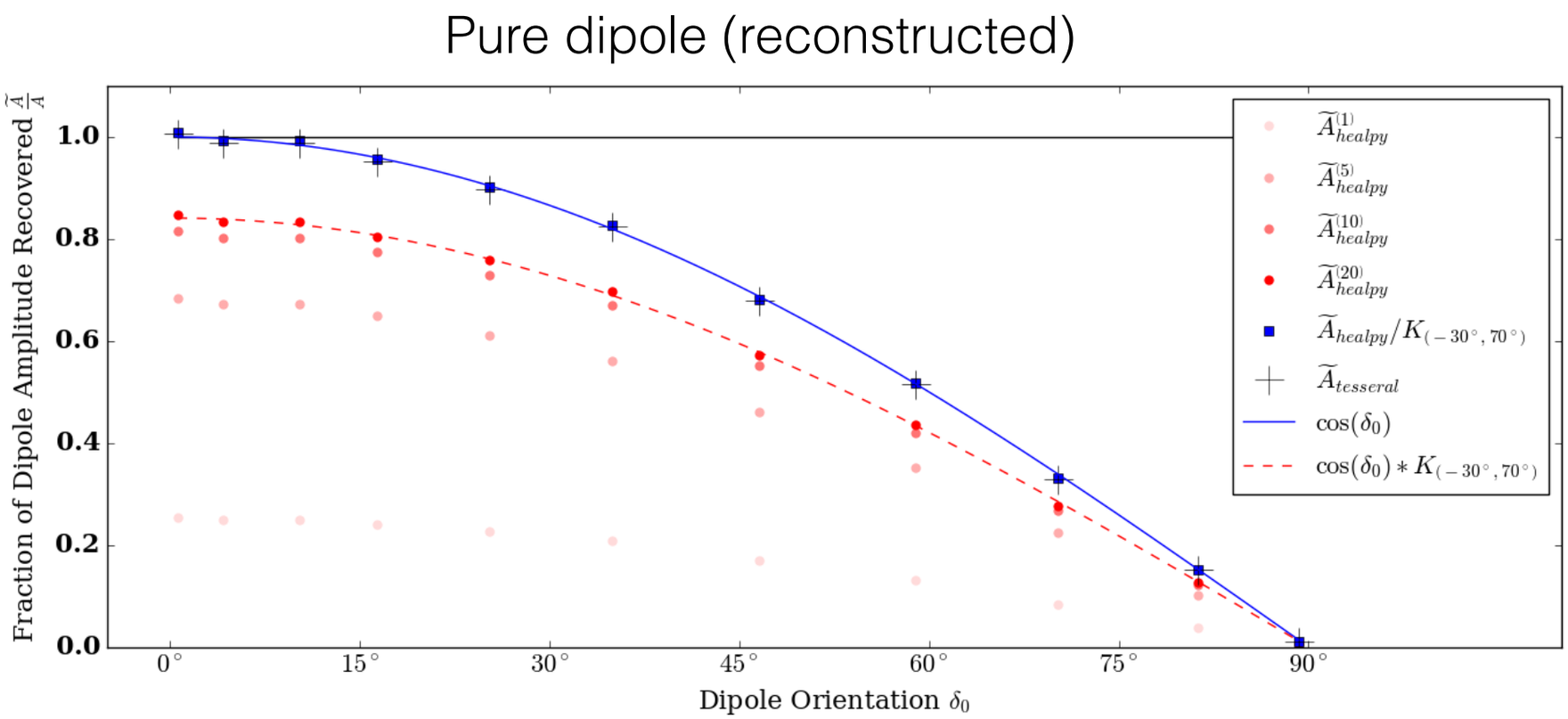

(A. U. Abeysekara, *et al.*, *in preparation*.)

- Simulated dipole reconstructed with LLH method.
- Blue line is best possible with ground-based observations.
- Method improves with iteration (light to dark red).
- Geometric correction needed due to limited sky coverage.

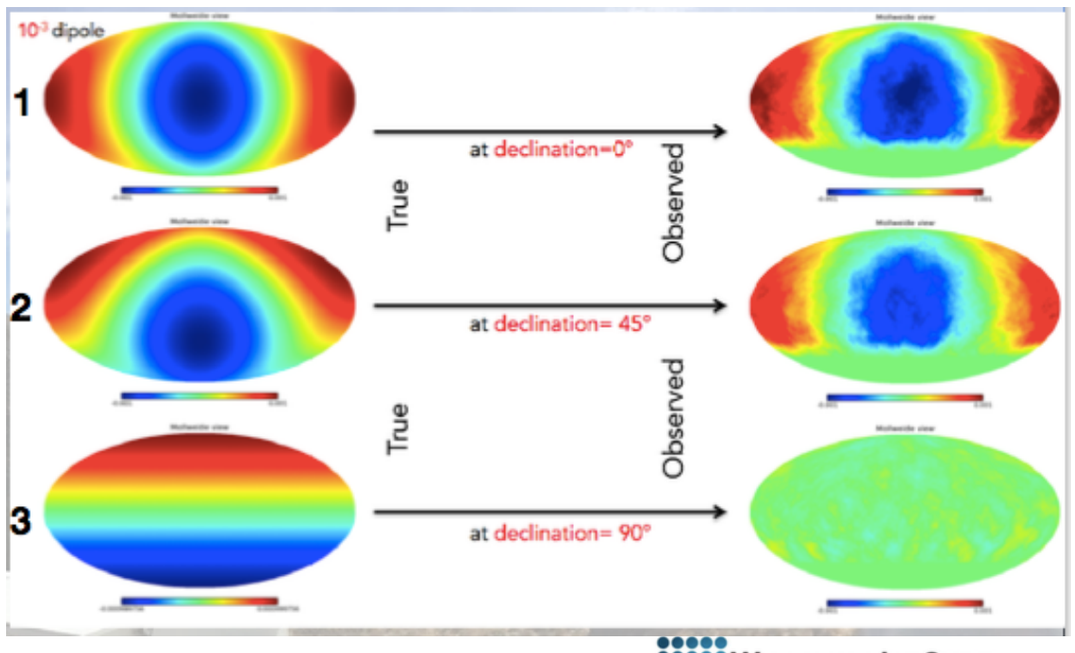

Partial sky-coverage

Pure dipole (3d sensitivity)

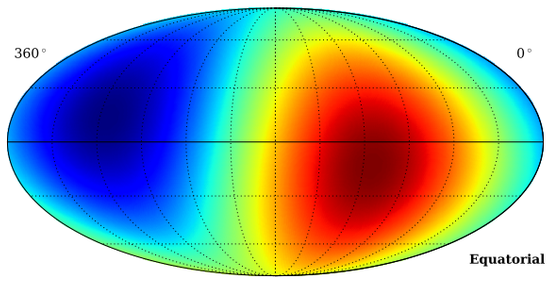

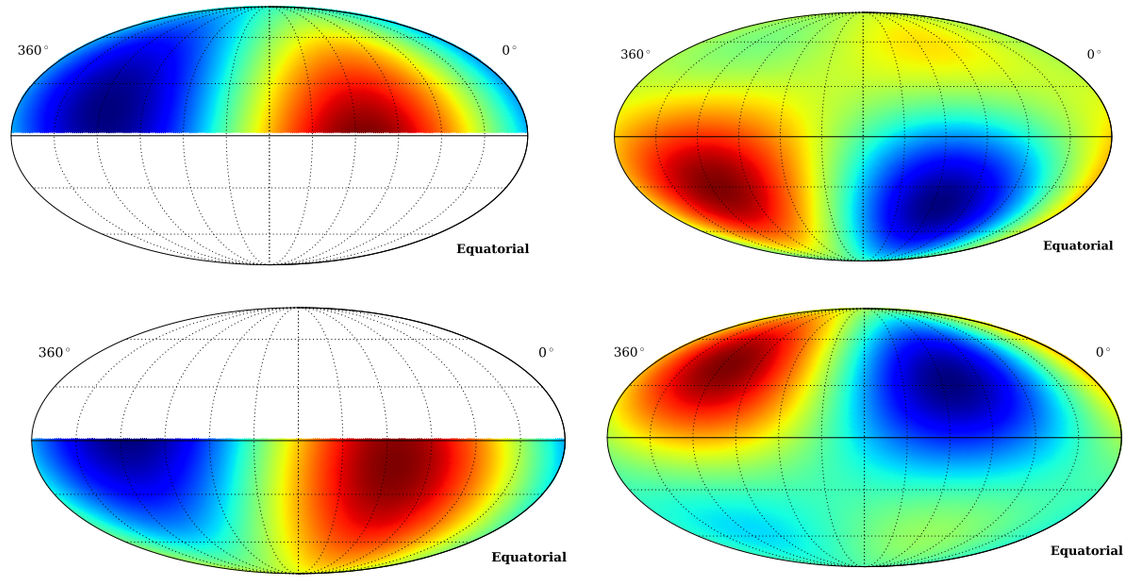

Multipole components are subject to crosstalk caused by partial sky coverage since there is a degeneracy between different ℓ-modes.

A purely dipole can result in an artificial quadrupole due to partial sky coverage.

Relative Intensity

Significance Map

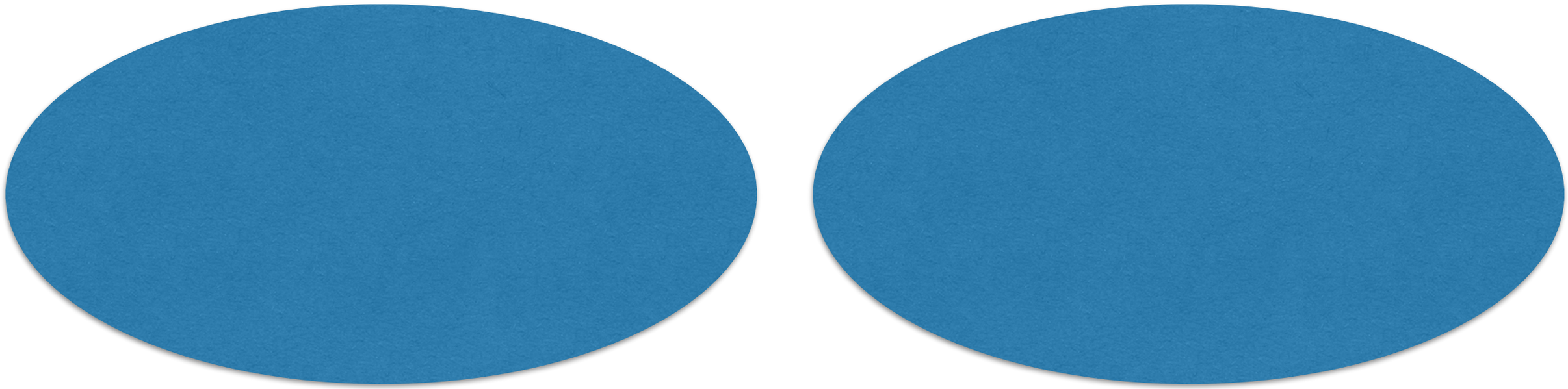

- Relative intensity and significance maps after 20 iterations smoothed over 5° radius.
- First full-sky combined observation at same energy with two observatories covering most of the celestial sphere.
- Significance of features in the northern sky is improved compared to maps presented at ICRC.

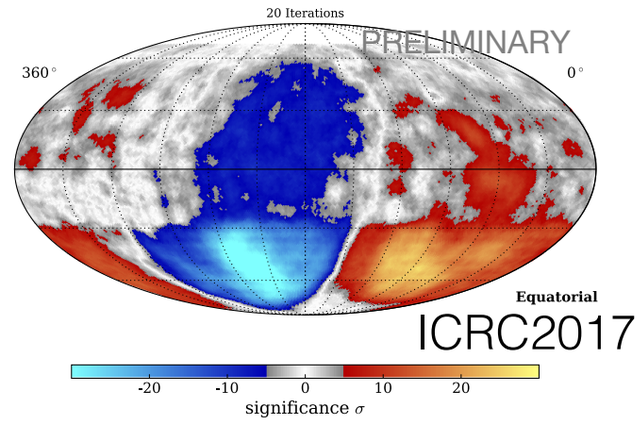

Overlapping Region

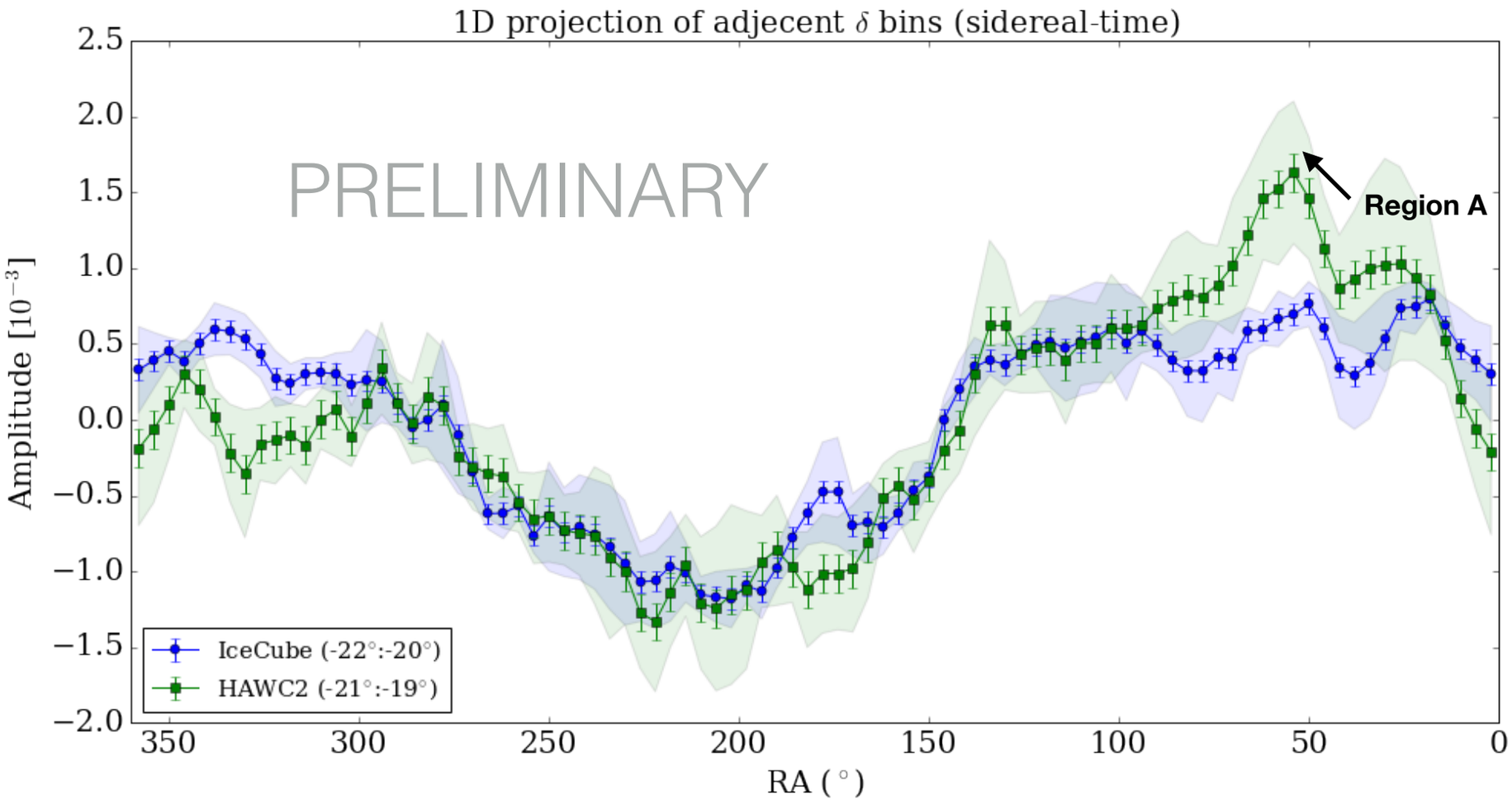

- Adjacent, overlapping δ bins at -20° for HAWC-300 and IC86 data.
- There is general agreement for large scale structures.
- The two curves correspond to different δ bands but some differences in the small scale structure might also be attributed to mis-reconstructed events that migrate from nearby δ bins with larger statistics as well as possible energy and composition differences.

Angular Power Spectrum

The angular pseudo-power spectrum of the cosmic ray anisotropy for the combined IceCube and HAWC dataset. The red dots correspond to the power spectrum resulting from subtracting the fit to the large scale features ($\ell = 1, 2, 3$). The gray band represent the power spectra for isotropic sky maps at the 90% confidence level. The structure appears to have a very steep spectrum at low ℓ and a flatter spectrum at $\ell > 3$.

- Iterative method recovers most of the power of large scale structure in mid-latitude observatories like HAWC.
- No appreciable gain for IceCube.
- The highest angular power for $\ell = 1$ is obtained with the greater sky coverage from combining data from both observatories and reconstruction with the iterative method.

Angular Power Spectrum

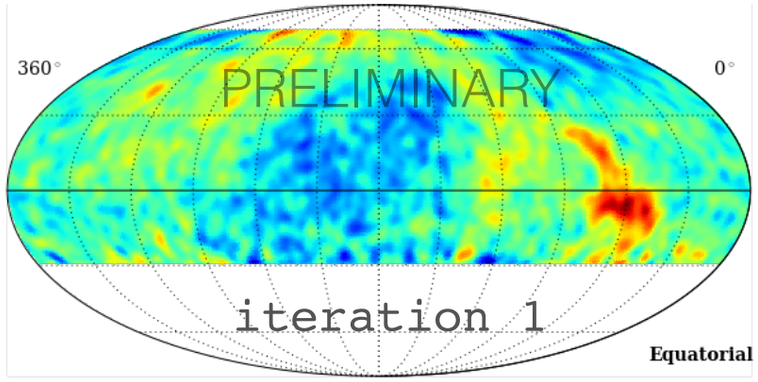

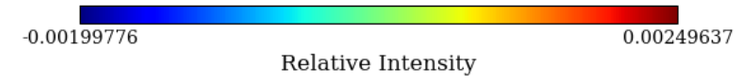

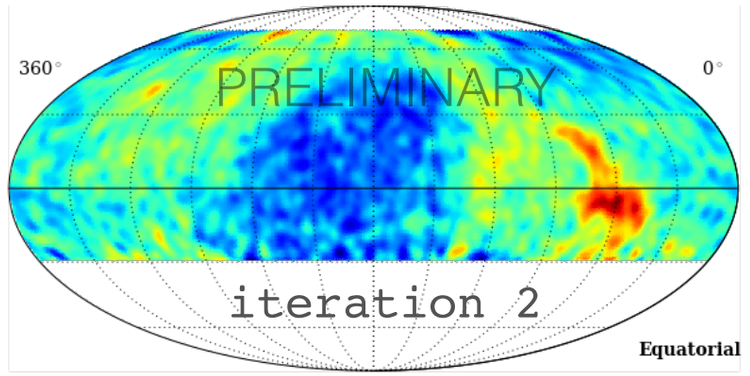

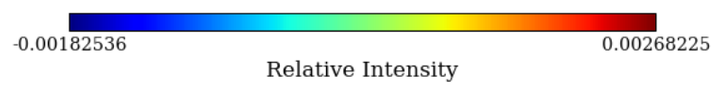

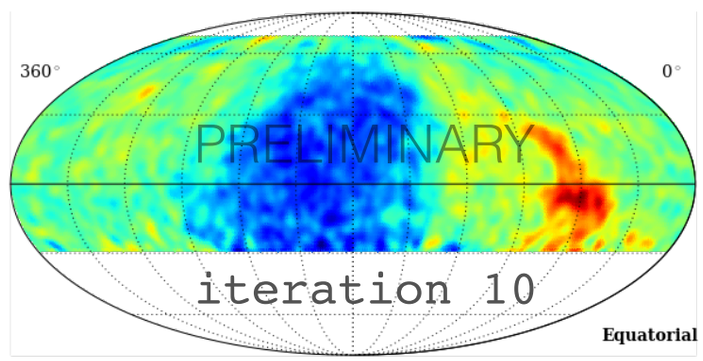

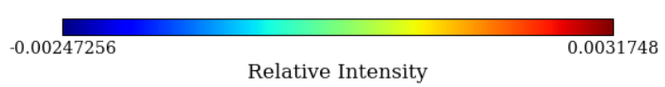

2D Fit

Summary plot (adopted from M. Ahlers et al. ArXiv:1612.01873) of the reconstructed TeV-PeV dipole amplitude and phase.

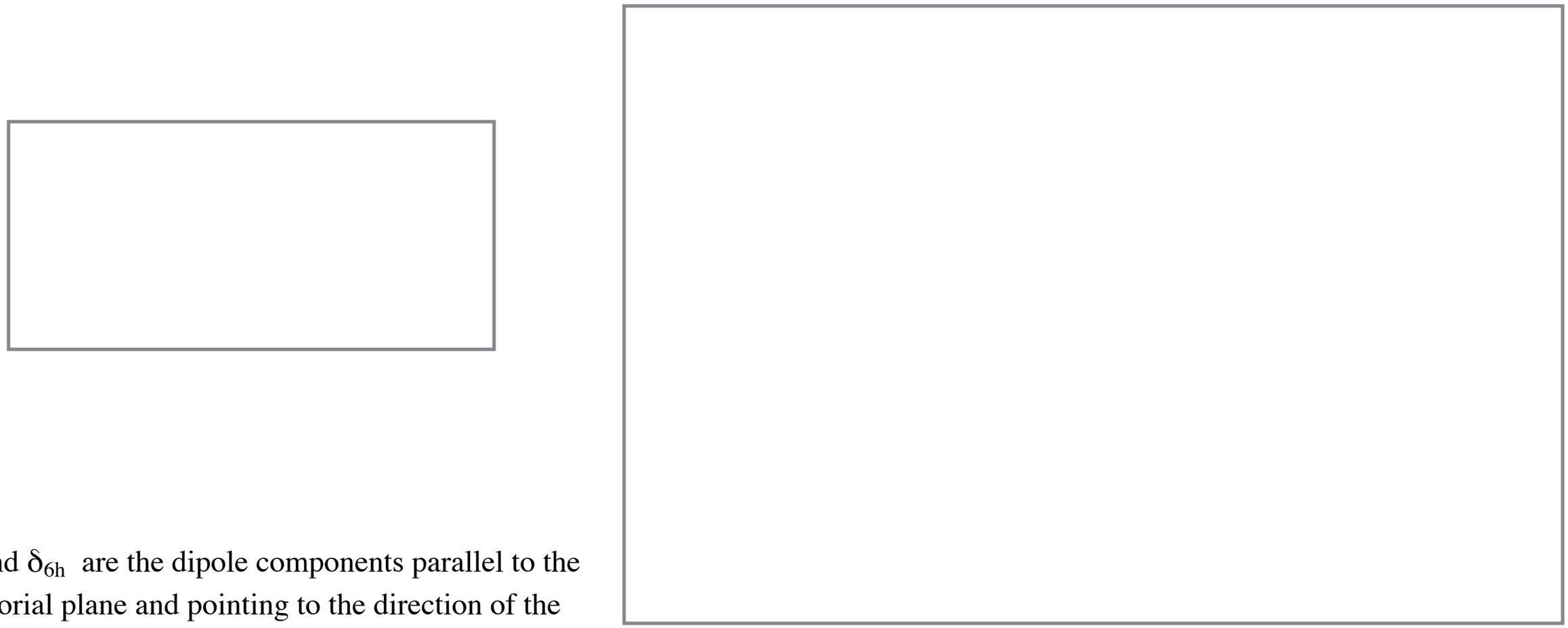

δ_{0h} and δ_{6h} are the dipole components parallel to the equatorial plane and pointing to the direction of the local hour angle 0h ($\alpha = 0^{\circ}$) and 6h ($\alpha = 90^{\circ}$) of the vernal equinox, respectively. The dipole component pointing north δ_N can not be constrained for ground-based observatories.

Small-scale Anisotropy

Multipole fit

Compton-Getting

Not from movement of Sun around Galactic center but through ISM

$v_{ISM} \simeq 23.2$ km/s in towards ($l \simeq 5.25^{o}$, $b \simeq 12.0^{o}$)

McComas et al. Science 336 (2012) 1291

Phase diagram in polar coordinates.

The amplitude corresponds to the radial distance while the phase corresponds to the angle in the counter-clockwise direction of the x-axis.

The values calculated in the figure take into account and subtract the contribution of the Compton-Getting effect which is estimated at a magnitude of 4.5×10^{-4} and pointing in the direction of 6h.

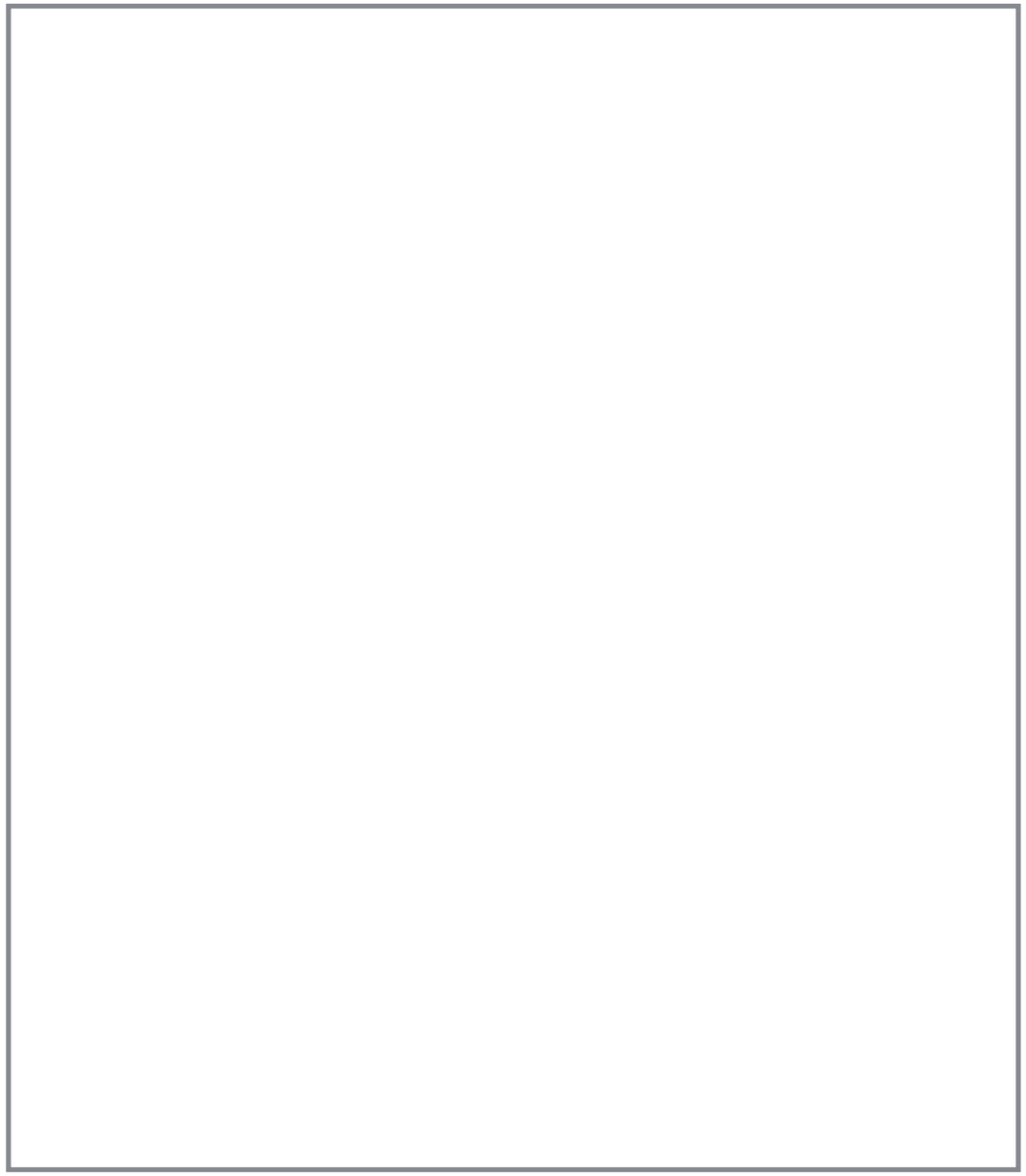

adopted from M. Ahlers et al. ArXiv:1612.01873

C-G corrected values:

Emerging model

1. Nearby sources of cosmic rays can introduce a contribution to the cosmic ray anisotropy depending on the age of the source, distance, magnetic connection and the diffusion of particles from these sources. These factors make the anisotropy sensitive to the energy of the particle.

2. The Compton-Getting effect: an apparent dipole due to the movement of the solar system within the Galaxy and the local environment and the effect of it on the intensity of the cosmic rays.

3. The LIMF appears to influence and reshape LS features.

4. The propagation of cosmic rays through the turbulent magnetic fields and the dispersion produced by sudden changes in the angle of passage with respect to the velocity of the particle and the magnetic field.

5. The propagation of cosmic rays through the magnetic and electric field of the heliosphere: large-scale dipole anisotropy patterns can be distorted, resulting in small structures observed.

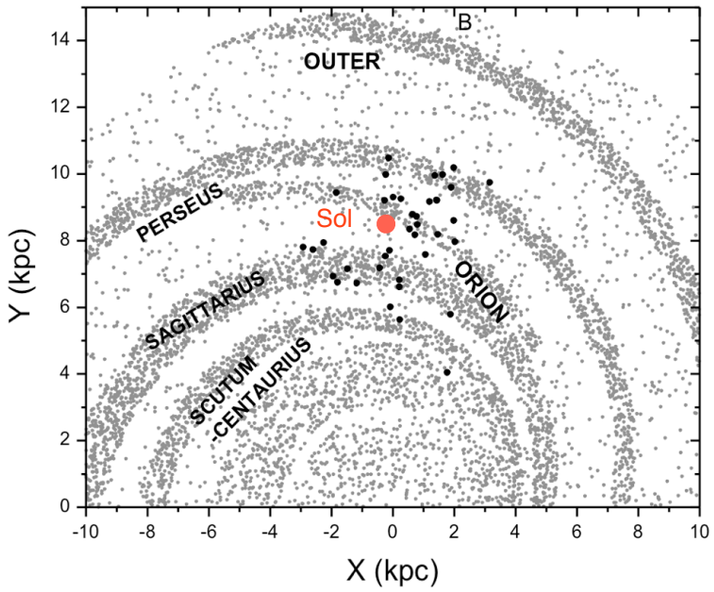

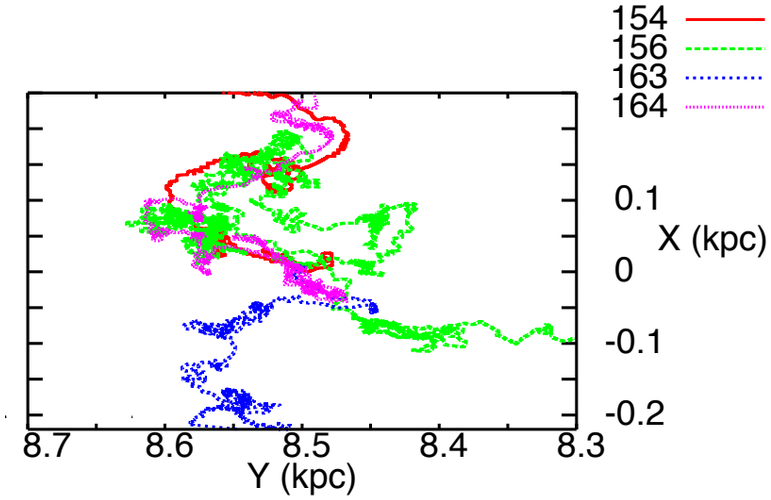

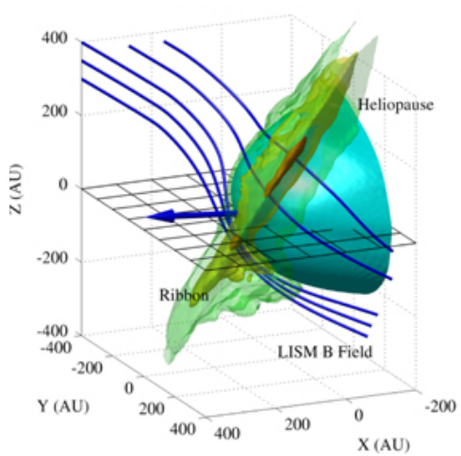

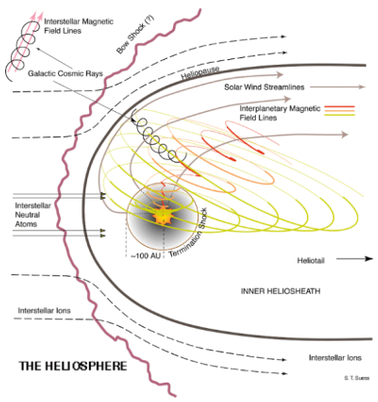

Summary

- **This IceCube-HAWC study is the first (nearly) full-sky cosmic ray arrival direction distribution analysis with combined data from observatories in the North and South at the same primary energy of 10 TeV and is a key to probe into the origin of the CRA observations.**

- Iterative maximum-likelihood reconstruction method simultaneously fits CR anisotropies and detector acceptance.

- Provides an optimal anisotropy reconstruction and the recovery of the dipole anisotropy for ground-based observatories located in middle latitudes.

- Ground-based observatories are generally insensitive to cosmic-ray anisotropy variations that are symmetric in RA, i.e. only vary across declination bands (i. e. dipole only observed as a projection onto celestial equator).

- Nearly full-sky coverage gives better fit of phase and amplitude of horizontal component of the dipole anisotropy.

- Small- and large-scale structures at 10 TeV appear to be qualitatively related with the local interstellar magnetic field and it's interaction with the structure of the heliosphere.

IceCube
SOUTH POLE NEUTRINO OBSERVATORY

HAWC
High Altitude Water Cherenkov
Gamma-Ray Observatory

Merci

Backup

IC86 2011-2016

- Data duration:
  - 5 continuous years
  - 2011-05-13 to 2016-05-20.
- Reconstructed a South Pole with fast but not very precise algorithms before being transmitted.
- Select long tracks with better angular reconstruction.
- Reconstructed energy < 32 TeV.

Data Cuts

- $\log_{10}(\mathbf{E}_{reco}) < 4.5$ (32 TeV)
- rlogl* < 15
- ldir_c** > 200 $\cos(\boldsymbol{\Theta}_{zenith})$
- ndir_c*** > 9 $\cos(\boldsymbol{\Theta}_{zenith})$

*Reduced log-likelihood of the track reconstruction fit.
**Length of track in direct (on-time) PE hits.
***Number of direct (on-time) PE hits.

HAWC300 2015-2017

- Data duration:
  - 519.0 cont. day periods (653 total days)
  - 2015-05-01 to 2017-05-01
- Select high quality reconstructions.
- Eliminate $\boldsymbol{\gamma}$-ray candidate events
- Reconstructed energy > 7.24 TeV.

Data Cuts

- $\log_{10}(\mathbf{E}_{reco}) >= 3.86$ (7.24 TeV)
- nHit* >= 75
- $0 \leq \boldsymbol{\Theta}_{zenith} < 1.0$ (57.3°)
- CxPE40XnCh** > 40
- PINC*** > 1.8

*Number of PE hits.
**Number of channels beyond 40m from the reconstructed core.
***Gamma/Hadron separation (smoothness of shower).

Large-scale Anisotropy (LIMF)

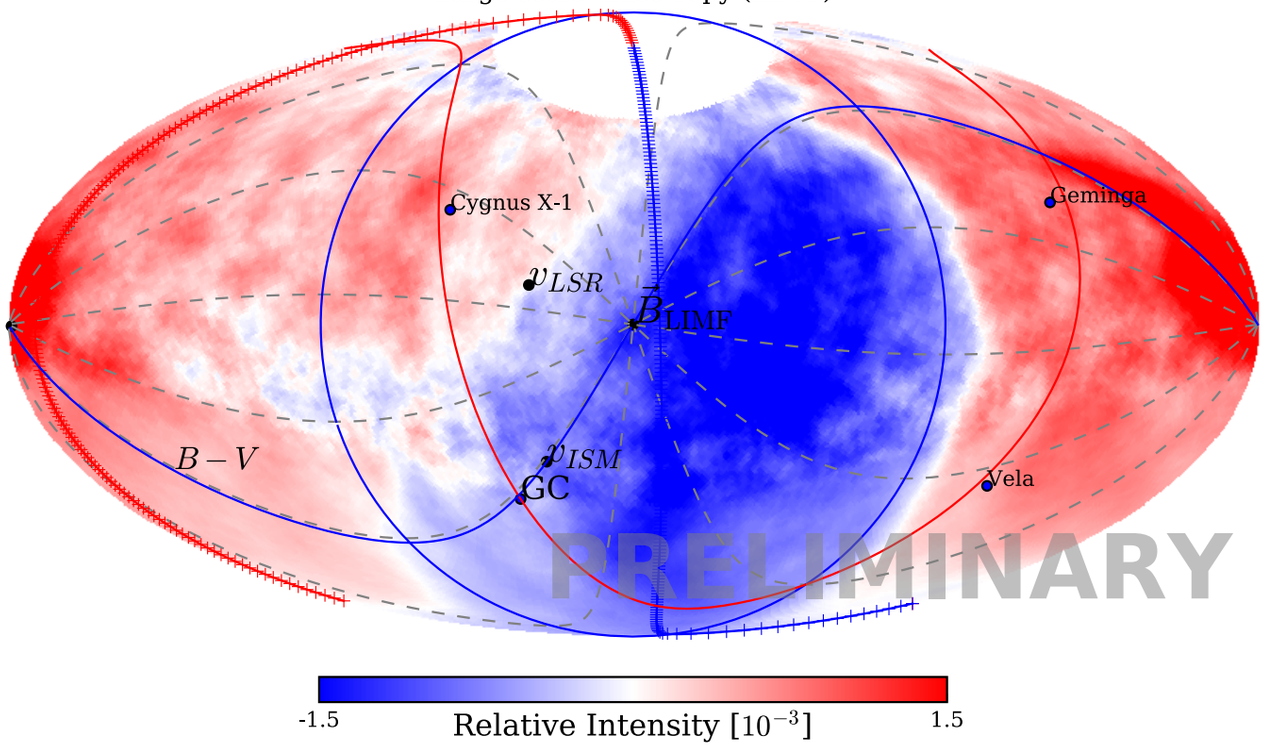

-1.5 Relative Intensity [10^{-3}] 1.5

Large-scale Anisotropy (Anti-LIMF)

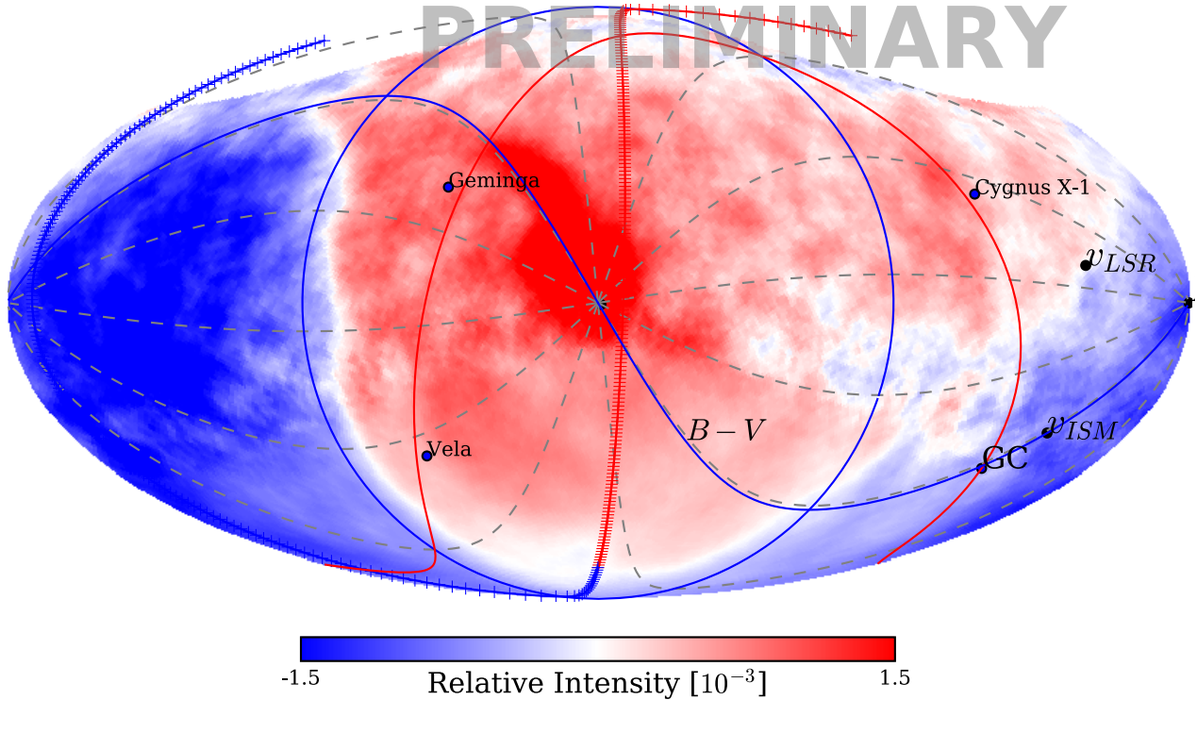

-1.5 Relative Intensity [10^{-3}] 1.5

Small-scale Anisotropy (LIMF)

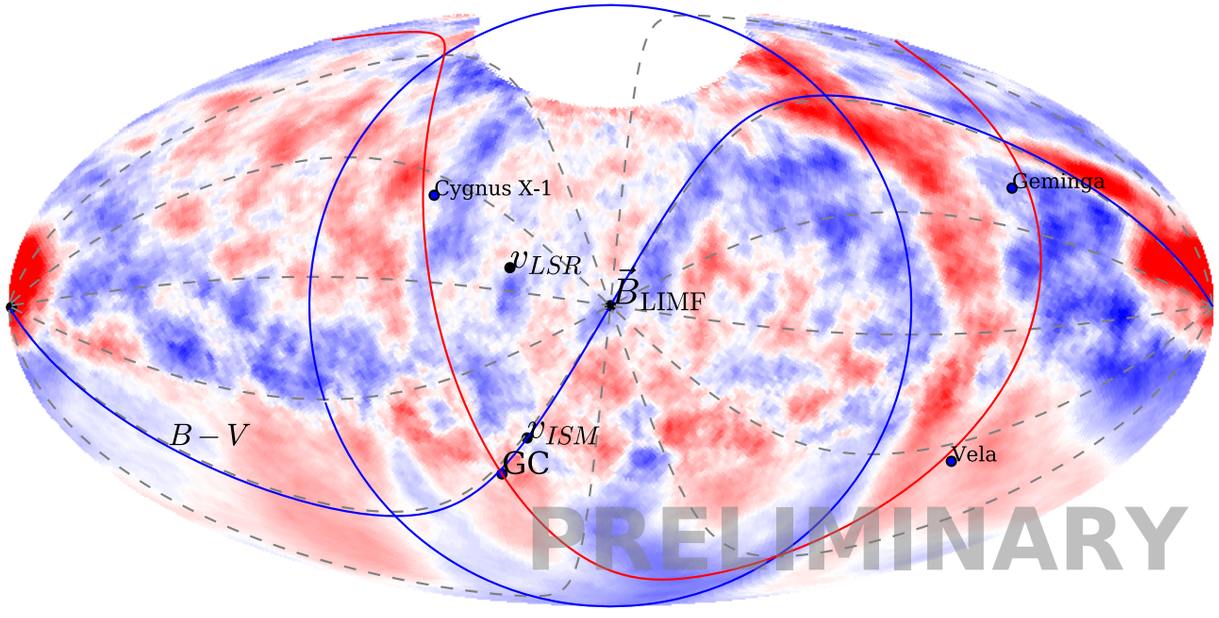

-0.8 Relative Intensity [10^{-3}] 0.8

Small-scale Anisotropy (Anti-LIMF)

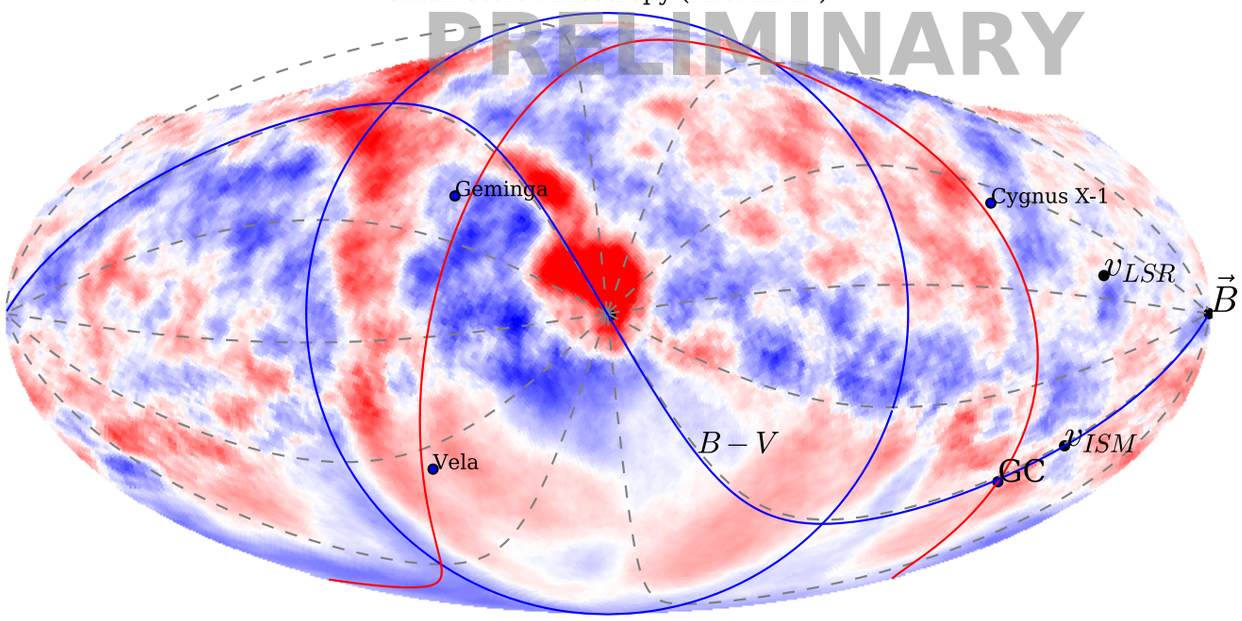

-0.8 Relative Intensity [10^{-3}] 0.8

Generalization for multiple observatories

In the case where you have multiple observations with common pixels, the optimal fit of the relative acceptance $\mathscr{A}$ (0) and the background rate $\mathscr{N}$ (0) of the null hypothesis becomes

$$\mathcal{N}_\tau^{s\,(0)} = \sum_i w_i^s n_{\tau i}\,, \qquad \mathcal{A}_i^{s\,(0)} = \sum_\tau w_i^s n_{\tau i} \Big/ \sum_{\kappa j} w_j^s n_{\kappa j}\,.$$

Where ***s*** corresponds to the index of the observatory.

Then the maximum of the signal hypothesis obeys the implicit relation

$$I_{\mathfrak{a}}^\star = \sum_\tau n_{\tau\mathfrak{a}} \Big/ \sum_{s\kappa} \mathcal{A}_{\kappa\mathfrak{a}}^{s\,\star} \mathcal{N}_\kappa^{s\,\star}\,,$$

$$\mathcal{N}_\tau^{s\,\star} = \sum_i w_i^s n_{\tau i} \Big/ \sum_j \mathcal{A}_j^{s\,\star} I_{\tau j}^\star\,,$$

$$\mathcal{A}_i^{s\,\star} = \sum_\tau w_i^s n_{\tau i} \Big/ \sum_\kappa \mathcal{N}_\kappa^{s\,\star} I_{\kappa i}^\star\,.$$